

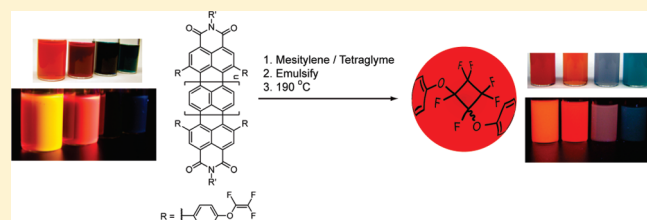
## Thermally Polymerized Rylene Nanoparticles

Trisha L. Andrew and Timothy M. Swager\*

Department of Chemistry, Massachusetts Institute of Technology, 77 Massachusetts Avenue, Cambridge, Massachusetts 02139, United States

Supporting Information

**ABSTRACT:** Rylene dyes functionalized with varying numbers of phenyl trifluorovinyl ether (TFVE) moieties were subjected to a thermal emulsion polymerization to yield shape-persistent, water-soluble chromophore nanoparticles. Perylene and terrylene diimide derivatives containing either two or four phenyl TFVE functional groups were synthesized and subjected to thermal emulsion polymerization in tetraglyme. Dynamic light scattering measurements indicated that particles with sizes ranging from 70 to 100 nm were obtained in tetraglyme, depending on monomer concentration. The photophysical properties of individual monomers were preserved in the nanoemulsions, and emission colors could be tuned between yellow, orange, red, and deep red. The nanoparticles were found to retain their shape upon dissolution into water, and the resulting water suspensions displayed moderate to high fluorescence quantum yield.



## INTRODUCTION

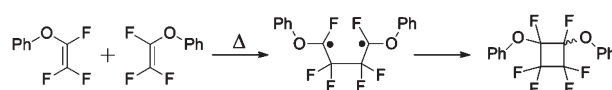
Chromophore and conjugated polymer (CP) nanoparticles and nanocomposites<sup>1</sup> have recently found prominence in various applications, including optoelectronics<sup>2</sup> and biological imaging and sensing.<sup>3</sup> In certain cases, CP nanoparticles displayed desirable properties that were either absent (water solubility) or not as prominent (two-photon absorption cross section) in CP thin films or solutions.<sup>3,4</sup> Additionally, there is considerable interest in using CP nanoparticles to improve or control the nanoscale composition of CP blends to improve the efficiency of polymer LEDs and photovoltaics.<sup>2,5</sup> Fluorescence energy transfer in small molecule chromophore-containing nanoparticles has also been investigated for live cell imaging.<sup>3e,6</sup>

CP nanoparticles are predominantly fabricated by microprecipitation methods, where a small aliquot of a dilute solution of the CP in a good solvent (such as tetrahydrofuran) is added to a poor solvent (such as water) with sonication.<sup>4</sup> In the case of small molecule chromophores, emulsions of monomers containing polymerizable functional groups are first formed (sometimes in the presence of surfactants), and then the monomers are polymerized within the microcapsules (using either radical initiators or metal catalysts) to yield shape-persistent chromophore or CP nanoparticles.<sup>7</sup> Rylene dyes, particularly 3,4,9,10-perylene tetracarboxydiimides (PDIs), are frequently used as the chromophore component owing to their brilliant colors, large extinction coefficients, near-unity fluorescence quantum yields, and remarkable photostability.<sup>8</sup> Recent examples of rylene-containing nanoparticles almost always utilize methacrylate-functionalized chromophores, which are then polymerized in microemulsions by established controlled radical polymerization processes.<sup>3c-e</sup>

Aryl trifluorovinyl ethers (TFVEs) are a unique class of molecules that have been shown to undergo a thermal dimerization

reaction to generate perfluorocyclobutane (PFCB) derivatives (Figure 1A).<sup>9</sup> Smith and co-workers have synthesized numerous, high molecular-weight polymers by thermally polymerizing monomers containing multiple TFVE moieties.<sup>10</sup> Moreover, because of the availability of a key synthetic intermediate (**1**, Figure 1B), the straightforward incorporation of phenyl TFVE moieties into a variety of chromophore skeletons is possible.<sup>11</sup> In the past decade, TFVE-containing chromophore thermosets have been explored as thermally stable nonlinear optical polymers,<sup>12</sup> optical waveguides,<sup>13</sup> and hole-transporting materials in organic light-emitting diodes.<sup>14</sup>

## (A)



## (B)

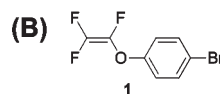


**Figure 1.** (A) Thermal dimerization reaction of aryl trifluorovinyl ethers (TFVEs), shown for phenyl TFVE. (B) Structure of 4-bromophenyl TFVE (**1**).

Thus far, the thermal, radical initiator-free fabrication of shape-persistent nanoparticles has not been demonstrated. We anticipated that the thermal reactivity of TFVEs would allow

Received: January 13, 2011

Revised: February 15, 2011

Published: March 15, 2011

access to such nanoparticles. Herein we describe the synthesis of rylene dyes functionalized with two or more phenyl TFVE moieties and the fabrication of rylene nanoparticles via a thermal emulsion polymerization.

## MATERIALS AND METHODS

**General Considerations.** Synthetic manipulations were carried out under argon using dry solvents and standard Schlenk techniques. All solvents were of ACS reagent grade or better unless otherwise noted. 1,4-Dioxane and 1,2-dimethoxyethane were purified by distillation over activated alumina. Silica gel (40–63  $\mu\text{m}$ ) was obtained from SiliCycle Inc.  $\text{Pd}_2(\text{dba})_3 \cdot \text{CHCl}_3$  and S-Phos were purchased from Strem Chemicals and used without further purification. Tetraglyme was purchased from VWR and purified by passing through a plug of activated neutral alumina. Compounds **2**,<sup>15</sup> **3**,<sup>9c</sup> **4**,<sup>16</sup> **5**,<sup>9c</sup> and **6**<sup>17</sup> were synthesized following published procedures. Ultraviolet–visible absorption spectra were measured with an Agilent 8453 diode array spectrophotometer and corrected for background signal with a solvent-filled cuvette. Fluorescence spectra were measured on a SPEX Fluorolog-t3 fluorimeter (model FL-321, 450 W xenon lamp) using right-angle detection. Fluorescence lifetimes were measured via frequency modulation using a Horiba-Jobin-Yvon MF2 lifetime spectrometer equipped with a 365 nm laser diode and using the modulation of POPOP as a calibration reference. Mesitylene/tetraglyme biphasic mixtures were emulsified with either an IKA Ultra-Turrax T25 Basic high-shear disperser (at a shear rate of 24/min) or a Mixonix Microson ultrasonic cell disruptor. DLS measurements were performed at the MIT Biophysics Instrumentation Facility using a Wyatt Technologies DynaPro Titan dynamic light scatterer equipped with a 830 nm diode laser. Data were fitted to a globular protein model, taking into account solvent refractive indices and viscosities ( $\text{CHCl}_3$ : 0.57 cP at 20 °C; toluene: 0.59 cP at 20 °C; tetraglyme: 4.1 cP at 20 °C; water: 1.00 cP at 20 °C).

**General Procedure for the Synthesis of M1, M2, and M4.** A flame-dried 50 mL Schlenk flask was charged with the appropriate rylene bromide, **3** (1.5 equiv per bromine substituent),  $\text{Pd}_2(\text{dba})_3 \cdot \text{CHCl}_3$  (0.05 equiv), S-Phos (0.2 equiv), and anhydrous potassium phosphate (20 equiv) under a positive flow of argon. Dry, degassed 1,2-dimethoxyethane (15 mL) was introduced via cannula addition, and the resulting mixture was heated at 60 °C for 12 h. The reaction was cooled to room temperature and passed through a Celite plug, and the solvent evaporated under reduced pressure. The resulting residue was purified by flash column chromatography using 50/50 hexanes/dichloromethane as the eluent.

**M1.** Isolated in 70% as a deep red solid from **2** following the procedure described above, with the substitutions of 1,4-dioxane for 1,2-dimethoxyethane and 3.0 M aqueous potassium phosphate for anhydrous potassium phosphate.  $^1\text{H}$  NMR (400 MHz,  $\text{CDCl}_3$ ,  $\delta$ ): 8.56 (s, 2H), 8.18 (d,  $J = 8.4$  Hz, 2H), 7.80 (d,  $J = 8.4$  Hz, 2H), 7.56 (d,  $J = 8.0$  Hz, 4H), 7.23 (d,  $J = 8.0$  Hz, 4H), 4.11 (m, 4H), 1.92 (m, 2H), 1.55 (s, 6H), 1.32 (m, 20H), 0.91 (m, 14H).  $^{13}\text{C}$  NMR (100 MHz,  $\text{CDCl}_3$ ,  $\delta$ ): 163.8, 139.9, 139.4, 136.8, 136.1, 135.0, 131.1, 130.3, 130.1, 129.8, 128.6, 122.5, 121.4, 117.8, 44.5, 38.1, 30.9, 28.9, 24.2, 23.2, 14.3, 10.8.  $^{19}\text{F}$  NMR (376 MHz,  $\text{CDCl}_3$ ,  $\delta$ ): -119.00 (dd,  $J = 98$ , 60 Hz, 1F), -126.69 (dd,  $J = 109$ , 98 Hz, 1F), -134.47 (dd,  $J = 109$ , 60 Hz, 1F). UV–vis ( $\text{CHCl}_3$ ):  $\lambda_{\text{max}}$  ( $\log \epsilon$ ) = 400 (3.8), 475 (3.2), 519 (4.0), 553 (4.4). HRMS (ESI,  $m/z$ ):  $[\text{M} + \text{H}]^+$  calcd for  $\text{C}_{56}\text{H}_{49}\text{F}_6\text{N}_2\text{O}_6$ , 959.3495; found, 959.3493.

**M2.** Isolated in 50% as a deep red solid from **2** following the procedure described above.  $^1\text{H}$  NMR (400 MHz,  $\text{CDCl}_3$ ,  $\delta$ ): 8.29 (s, 4H), 7.56 (d,  $J = 8.0$  Hz, 8H), 7.23 (d,  $J = 8.0$  Hz, 8H), 4.11 (m, 4H), 1.92 (m, 2H), 1.55 (s, 6H), 1.32 (m, 20H), 0.91 (m, 14H).  $^{13}\text{C}$  NMR (100 MHz,  $\text{CDCl}_3$ ,  $\delta$ ): 163.7, 139.8, 139.4, 136.8, 135.8, 135.0, 131.1, 130.3, 130.1, 128.6, 122.5, 121.4, 117.8, 44.5, 38.1, 30.9, 28.9, 24.2, 23.2, 14.3, 10.8.  $^{19}\text{F}$  NMR (376 MHz,  $\text{CDCl}_3$ ,  $\delta$ ): -119.00 (dd,  $J = 98$ , 60 Hz,

1F), -126.69 (dd,  $J = 109$ , 98 Hz, 1F), -134.47 (dd,  $J = 109$ , 60 Hz, 1F). UV–vis ( $\text{CHCl}_3$ ):  $\lambda_{\text{max}}$  ( $\log \epsilon$ ) = 400 (3.8), 558 (4.0), 592 (4.3). HRMS (ESI,  $m/z$ ):  $[\text{M} + \text{H}]^+$  calcd for  $\text{C}_{72}\text{H}_{55}\text{F}_{12}\text{N}_2\text{O}_8$ , 1303.3767; found, 1303.3769.

**M4.** Isolated in 74% as a greenish-blue solid from **6** following the procedure described above.  $^1\text{H}$  NMR (400 MHz,  $\text{CDCl}_3$ ,  $\delta$ ): 8.37 (s, 4H), 7.98 (s, 4H), 7.56 (d,  $J = 8.4$  Hz, 8H), 7.27 (t,  $J = 4.8$  Hz, 2H), 7.23 (d,  $J = 8.4$  Hz, 8H), 7.01 (d,  $J = 4.8$  Hz, 4H), 2.68 (m, 4H), 1.08 (s, 24H).  $^{13}\text{C}$  NMR (100 MHz,  $\text{CDCl}_3$ ,  $\delta$ ): 163.3, 155.0, 153.2, 147.8, 145.8, 134.6, 132.1, 132.0, 129.7, 129.2, 129.2, 129.0, 128.9, 128.4, 127.4, 127.3, 126.1, 125.8, 125.5, 124.1, 123.4, 122.7, 122.0, 119.3, 34.7, 29.2, 21.6.  $^{19}\text{F}$  NMR (376 MHz,  $\text{CDCl}_3$ ,  $\delta$ ): -119.00 (dd,  $J = 98$ , 60 Hz, 1F), -126.69 (dd,  $J = 109$ , 98 Hz, 1F), -134.47 (dd,  $J = 109$ , 60 Hz, 1F). UV–vis ( $\text{CHCl}_3$ ):  $\lambda_{\text{max}}$  ( $\log \epsilon$ ) = 410 (3.0), 610 (3.1), 665 (3.7), 720 (3.9). HRMS (ESI,  $m/z$ ):  $[\text{M} + \text{H}]^+$  calcd for  $\text{C}_{90}\text{H}_{59}\text{F}_{12}\text{N}_2\text{O}_8$ , 1523.4080; found, 1523.1520.

**General Procedure for the Synthesis of M3 and M5.** A flame-dried 50 mL Schlenk flask was charged with the appropriate rylene bromide, **5** (1.1 equiv per bromine substituent), and anhydrous potassium carbonate (1.1 equiv per bromine substituent) under a positive flow of argon. Dry, degassed *N*-methyl-2-pyrrolidone (10 mL) was introduced via cannula addition, and the resulting mixture was heated at 80 °C for 12 h. The reaction was cooled to room temperature, diluted with 1 M HCl, and extracted with  $\text{CHCl}_3$  ( $3 \times 30$  mL). The organic layers were combined and dried over magnesium sulfate, and the solvent evaporated under reduced pressure. The resulting residue was purified by flash column chromatography using 60/40 hexanes/dichloromethane as the eluent.

**M3.** Isolated in 85% as a deep red solid from **4** following the procedure described above.  $^1\text{H}$  NMR (400 MHz,  $\text{CDCl}_3$ ,  $\delta$ ): 9.47 (d,  $J = 8.4$  Hz, 2H), 8.57 (d,  $J = 8.4$  Hz, 2H), 8.23 (s, 1H), 7.18 (m, 8H), 4.04 (m, 4H), 1.87 (m, 2H), 1.57 (s, 4H), 1.28 (m, 22H), 0.88 (m, 16H).  $^{13}\text{C}$  NMR (100 MHz,  $\text{CDCl}_3$ ,  $\delta$ ): 163.7, 155.3, 139.4, 132.1, 130.5, 129.3, 129.0, 125.3, 124.1, 123.9, 122.4, 121.3, 118.3, 44.5, 38.1, 30.9, 28.9, 24.2, 23.2, 14.3, 10.8.  $^{19}\text{F}$  NMR (376 MHz,  $\text{CDCl}_3$ ,  $\delta$ ): -119.00 (dd,  $J = 98$ , 60 Hz, 1F), -126.69 (dd,  $J = 109$ , 98 Hz, 1F), -134.47 (dd,  $J = 109$ , 60 Hz, 1F). UV–vis ( $\text{CHCl}_3$ ):  $\lambda_{\text{max}}$  ( $\log \epsilon$ ) = 400 (3.8), 461 (3.8), 502 (4.1), 536 (4.4). HRMS (ESI,  $m/z$ ):  $[\text{M} + \text{H}]^+$  calcd for  $\text{C}_{56}\text{H}_{49}\text{F}_6\text{N}_2\text{O}_8$ , 991.3393; found, 991.3398.

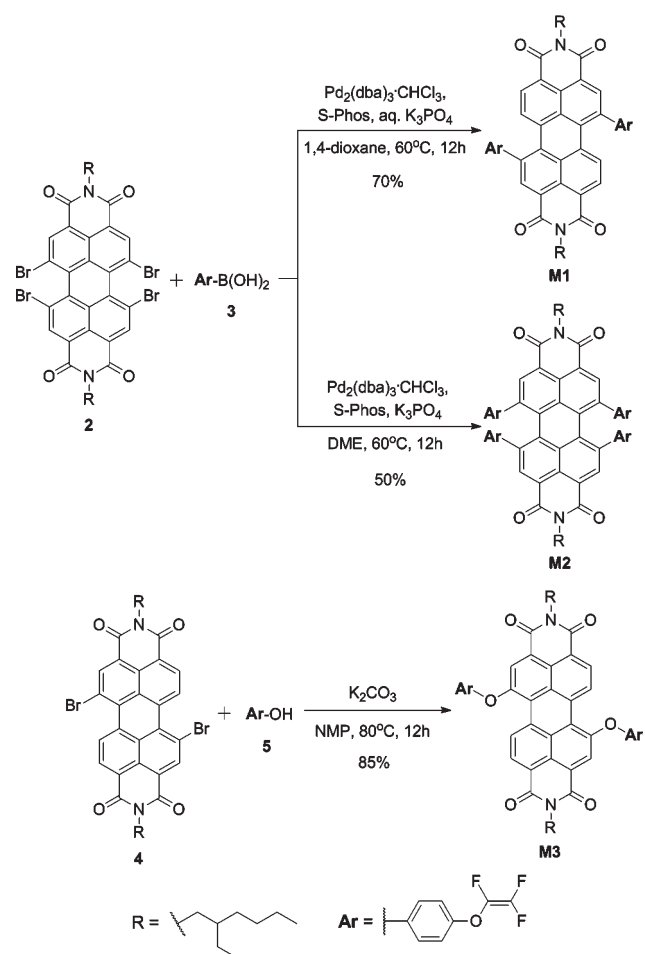
**M5.** Isolated in 87% as a deep blue solid from **6** following the procedure described above.  $^1\text{H}$  NMR (400 MHz,  $\text{CDCl}_3$ ,  $\delta$ ): 9.47 (s, 4H), 8.27 (s, 4H), 7.40 (d,  $J = 8.4$  Hz, 8H), 7.27 (t,  $J = 4.8$  Hz, 2H), 7.09 (d,  $J = 8.4$  Hz, 8H), 7.01 (d,  $J = 4.8$  Hz, 4H), 2.68 (m, 4H), 1.08 (s, 24H).  $^{13}\text{C}$  NMR (100 MHz,  $\text{CDCl}_3$ ,  $\delta$ ): 163.3, 155.0, 153.2, 147.8, 145.8, 134.6, 132.1, 132.0, 129.7, 129.2, 129.2, 129.0, 128.9, 128.4, 127.4, 127.3, 126.1, 125.8, 125.5, 124.1, 123.4, 122.7, 122.0, 119.3, 34.7, 29.2, 21.6.  $^{19}\text{F}$  NMR (376 MHz,  $\text{CDCl}_3$ ,  $\delta$ ): -119.00 (dd,  $J = 98$ , 60 Hz, 1F), -126.69 (dd,  $J = 109$ , 98 Hz, 1F), -134.47 (dd,  $J = 109$ , 60 Hz, 1F). UV–vis ( $\text{CHCl}_3$ ):  $\lambda_{\text{max}}$  ( $\log \epsilon$ ) = 410 (3.2), 569 (3.8), 623 (4.0), 680 (4.2). HRMS (ESI,  $m/z$ ):  $[\text{M} + \text{H}]^+$  calcd for  $\text{C}_{90}\text{H}_{59}\text{F}_{12}\text{N}_2\text{O}_{12}$ , 1587.3876; found, 1587.3877.

**Nanoparticle Synthesis.** 0.5 mL of a solution of the appropriate TFVE-functionalized rylene diimide monomer in mesitylene (0.2–1.6 mg/mL) was added to 5.0 mL of tetraglyme. The resulting biphasic mixture was either homogenized with a high-shear disperser or sonicated to yield a homogeneous emulsion, which was then heated to 190 °C under argon for 12 h.

## RESULTS AND DISCUSSION

**Monomer Synthesis.** PDIs were bay-functionalized with phenyl TFVE moieties starting from either tetrabromide **2**<sup>15</sup> or dibromide **4**<sup>16</sup> (Scheme 1). Following the previously reported synthesis and  $\text{CsF}/\text{Ag}_2\text{O}$ -mediated tetraarylation of **2**,<sup>15</sup> we

Scheme 1. Synthesis of Perylene Diimide-Containing Thermoset Monomers

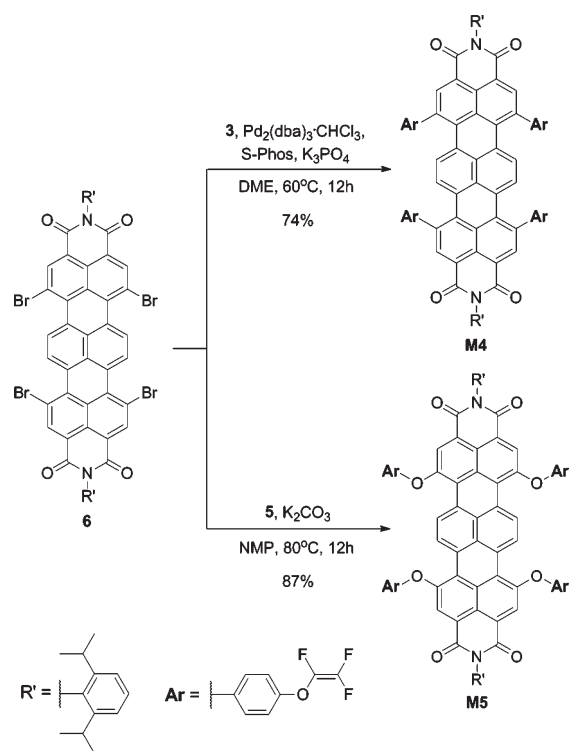


initially aimed to perform a 4-fold Suzuki–Miyaura coupling between **2** and **3**. However, the TFVE moiety was found to be slightly susceptible to nucleophilic addition of fluoride in the presence of the CsF/Ag<sub>2</sub>O base system, and the resulting hydro-1,2,2-fluoroethane-containing (–O–CHF–CF<sub>3</sub>) side products could not be separated from the reaction mixture. Instead, a 4-fold Suzuki–Miyaura cross-coupling under the modified Buchwald conditions was pursued. When aqueous potassium phosphate was employed as a base, tetrabromide **2** was partially dehalogenated and monomer **M1**, with two phenyl TFVE moieties, was isolated in 70% yield. Upon switching the base to rigorously anhydrous potassium phosphate, tetraarylated monomer **M2** was isolated in 50% yield. Taking advantage of the electron-deficient nature of the PDI skeleton, monomer **M3** was synthesized via an S<sub>N</sub>Ar reaction between **4** and **5**.<sup>17</sup>

The synthesis of TFVE-functionalized terrylene diimide (TDI) monomers is shown in Scheme 2. Similar to **M2**, the tetraarylated TDI monomer **M4** was synthesized starting from tetrabromide **6** via a modified Suzuki–Miyaura cross-coupling reaction with anhydrous potassium phosphate. Tetraaryloxy monomer **M5** was synthesized by an S<sub>N</sub>Ar reaction between **6** and **5**.

**Monomer Photophysics.** The photophysical properties of monomers **M1–5** (in CHCl<sub>3</sub> solutions) are summarized in Table 1. In general, the TFVE moieties were not observed to significantly affect the optical properties of rylene dyes. The absorption

Scheme 2. Synthesis of Terrylene Diimide-Containing Thermoset Monomers

Table 1. Photophysical Properties (in CHCl<sub>3</sub>) of Phenyl TFVE-Containing Rylene Diimides

compound	$\lambda_{\max}/\text{nm}$ (log $\epsilon$ )	$\lambda_{\text{em}}/\text{nm}$	$\Phi$	$\tau/\text{ns}$
<b>M1</b>	553 (4.4)	602	0.88 <sup>a</sup>	8.7
<b>M2</b>	592 (4.3)	640	0.61 <sup>a</sup>	9.8
<b>M3</b>	536 (4.4)	563	0.81 <sup>a</sup>	5.8
<b>M4</b>	720 (3.9)	765	0.08 <sup>b</sup>	5.7
<b>M5</b>	680 (4.2)	700	0.17 <sup>b</sup>	2.4

<sup>a</sup> Measured against Rhodamine B in ethanol ( $\Phi$  0.71). <sup>b</sup> Measured against zinc phthalocyanine in 1% pyridine in toluene ( $\Phi$  0.30).

and emission maxima and fluorescence quantum yields of monomers **M3** and **M5** were similar to phenyloxy-substituted PDI<sup>18a</sup> and TDI,<sup>18b</sup> respectively. Monomer **M2** displayed similar absorption and emission maxima to the previously reported tetraphenyl PDI. Consistent with similar observations for biphenyl-containing fluorophores,<sup>19</sup> phenyl substitution was found to increase the otherwise-small Stokes' shift of rylene dyes and decrease their fluorescence quantum yields. Moreover, the excited-state lifetimes of the phenyl-substituted rylenes, **M1**, **M2**, and **M4**, were found to be significantly longer than their parent rylene diimides (4.5 ns for *N*-(2-ethylhexyl)-PDI and 3.5 ns for *N*-(2,6-diisopropylphenyl)-TDI). These differences in photophysical properties are most likely caused by excited-state planarization across the biphenyl linkage.

**Nanoparticle Synthesis.** Rylene nanoparticles were synthesized by adding mesitylene solutions of monomers **M1–5** to tetraglyme and either homogenizing or sonicating the resulting biphasic system. This homogeneous mixture was then thermally cross-linked by heating to 190 °C for 12 h (Scheme 3). Scanning

## Scheme 3. Thermal Formation of Shape-Persistent Rylene Nanoparticles

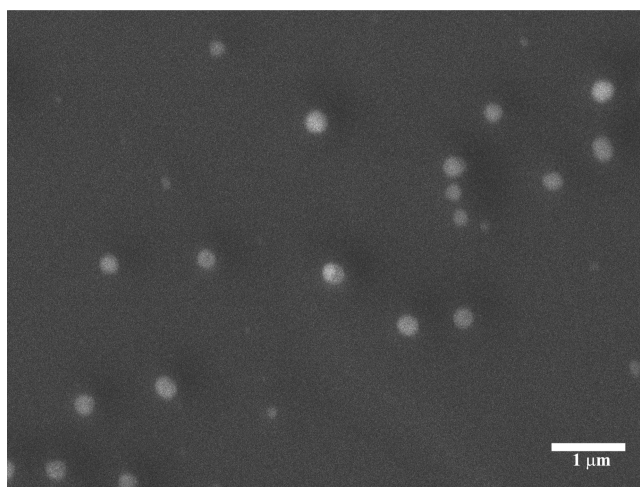
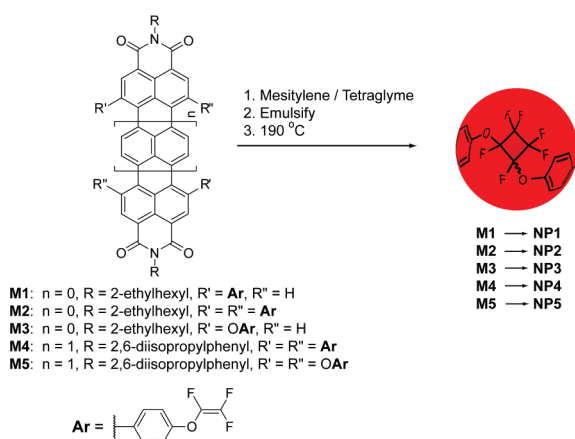


**Figure 2.** SEM micrograph of the thermally polymerized reaction mixture obtained from M2.

electron micrograph (SEM) images of the drop-cast reaction mixture thus obtained from M2 revealed the presence of poly-disperse, submicrometer particles (see Figure 2). Dynamic light scattering (DLS) measurements on the thermally polymerized mixtures fabricated from M1–5 indicated that particles with hydrodynamic radii between ca. 70 and 100 nm in tetraglyme were obtained (see Figure 3A). A significant difference was not observed in the size of the nanoparticles obtained from perylene (NP1–3) versus terrylene (NP4,5) diimide monomers. The size of the dye particles in tetraglyme could be controlled within the 70–100 nm range by varying the concentration of monomer in the starting mesitylene solution (see Figure 3B). DLS measurements indicated that NP1–5 did not coagulate in tetraglyme for at least 6 months (the stability of the nanoparticles as colloids in tetraglyme was only monitored for 6 months).

Once thermally polymerized, the chromophore nanoparticles could be extracted into organic solvents from the tetraglyme suspension.  $^{19}\text{F}$  NMR spectra of the *toluene-d*<sub>8</sub> extract of the thermally polymerized reaction mixture obtained from M2 indicated that the desired formation of PFCBs had proceeded, as the three characteristic doublet of doublets arising from the

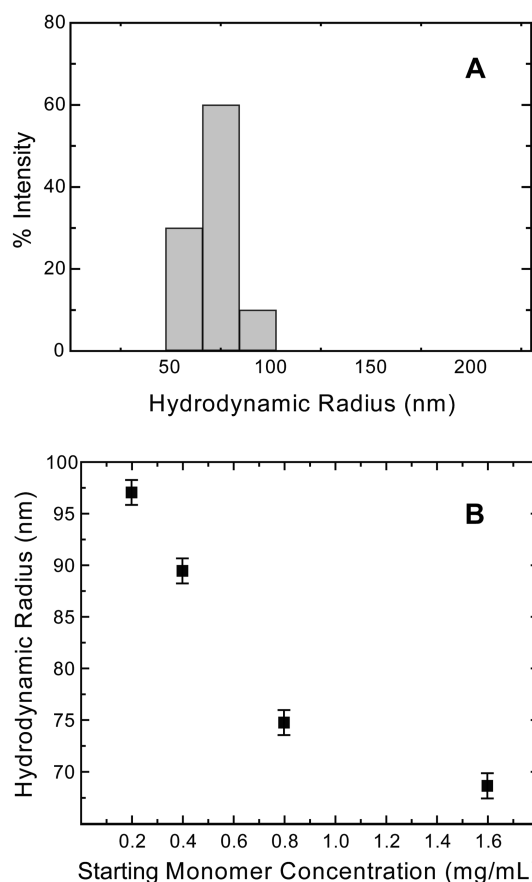


**Figure 3.** (A) Typical distribution of hydrodynamic radii in tetraglyme for the thermally polymerized mixtures fabricated with M1–5, as measured by dynamic light scattering (DLS); the particle size distribution for NP2 is shown (1.6 mg/mL starting monomer concentration in mesitylene). (B) Average hydrodynamic radii of particles obtained by varying the concentration of rylene monomer in the starting mesitylene solution (shown for NP2).

TFVE moiety<sup>9c</sup> were not observed (see Supporting Information). Additionally, undesired side products from the addition of water or other nucleophiles to the TFVE moiety were not evident in the  $^{19}\text{F}$  spectrum of NP2. Nanoparticles NP2, NP4, and NP5 were observed to retain their shape upon extraction into organic solvents (toluene and  $\text{CHCl}_3$ ); however, the hydrodynamic radii of these particles were observed to increase by  $\sim 30\%$  in organic solvents (see Figure 4). This is most likely due to swelling of the cross-linked nanoparticles by the organic solvents.

**Nanoparticle Photophysics.** The absorption and emission spectra of colloidal NP1–5 in tetraglyme (Figure 5A) were, overall, similar to those of their respective monomers in chloroform or toluene solutions, with two notable differences: the absorption and emission bands of the rylene nanoparticles were broadened and their emission maxima were hypsochromically shifted by  $\sim 15$  nm relative to their corresponding monomers. We tentatively ascribe these observations to aggregation of the rylene chromophores within individual nanoparticles, which is induced by the presence of trapped tetraglyme. Accordingly, the fluorescence quantum yields of the nanoparticles in tetraglyme were also slightly lower than those of the starting monomers—a ca. 5% loss in fluorescence quantum yield was generally observed after thermal emulsion polymerization in tetraglyme.

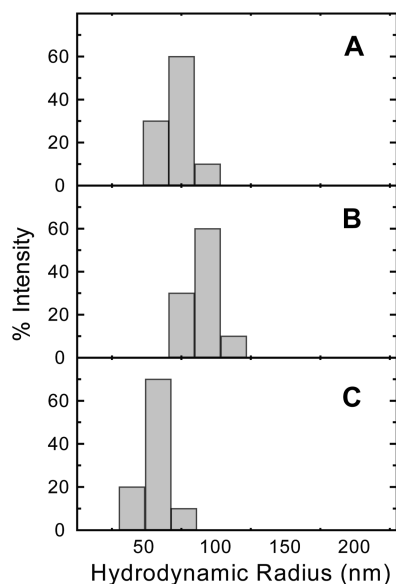


**Figure 4.** Typical changes in the measured hydrodynamic radii for NP2, NP4, and NP5 with changing solvents. The particle size distribution for NP2 (fabricated with 1.6 mg/mL starting monomer concentration in mesitylene) is shown in (A) tetraglyme, (B) toluene, and (C) water.

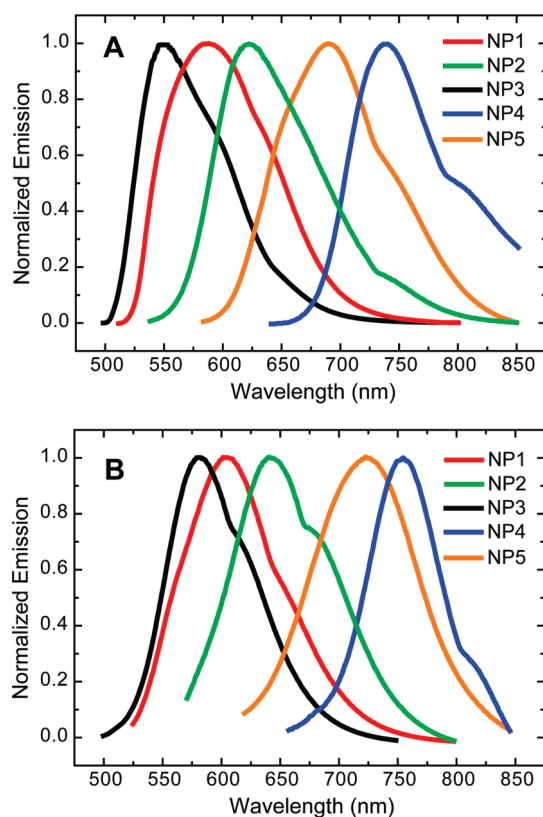


**Figure 5.** Emission spectra of NP1–5 as colloidal suspensions in tetraglyme (A) and as dilute suspensions in water (B, 1:50 dilution of the tetraglyme suspension into DI water).  $\lambda_{\text{ex}} = 480$  nm for NP1–3 and 580 nm for NP4,5.

The nanoparticle suspensions in tetraglyme were diluted into water (1:50 dilution), and the resulting aqueous mixtures were filtered through a 0.2  $\mu\text{m}$  PTFE filter to remove large aggregates.

The filtered aqueous solutions were homogeneous and nanoparticle precipitation was not evident by eye. DLS measurements revealed that the hydrodynamic radii of NP1–5 in water decreased by ca. 35% relative to those measured in tetraglyme (see Figure 4), most likely due to expulsion of trapped tetraglyme from within the nanoparticles. These aqueous solutions remained homogeneous by eye, and the measured hydrodynamic radii of the nanoparticles remained unchanged for at least 3 months. The emission spectra of NP1–5 in water are shown in Figure 5B. The emission maxima of NP1–5 in water are red-shifted relative to those in tetraglyme and are very similar to those of their corresponding monomers in chloroform solutions. In this case, we posit that the aforementioned expulsion of trapped tetraglyme from within the nanoparticles effectively reverses the aggregation-induced hypsochromic shifts observed in tetraglyme suspensions of NP1–5. Aqueous solutions of the perylene diimide nanoparticles NP1, NP2, and NP3 displayed good fluorescence quantum yields (63%, 50%, and 60%, respectively); however, the fluorescence quantum yields of aqueous solutions of the terrylene diimide nanoparticles NP4 and NP5 were relatively low (3% and 11%, respectively).<sup>20</sup>

## CONCLUSIONS

Rylene dyes functionalized with varying numbers of phenyl trifluorovinyl ether (TFVE) moieties were synthesized and subjected to a thermal emulsion polymerization to yield shape-persistent, water-soluble chromophore nanoparticles. The reported thermal emulsion polymerization is unique from previously reported methods to fabricate chromophore or conjugated polymer nanoparticles, as it does not involve the use of radical initiators or metal catalysts. Aqueous solutions of perylene diimide-containing nanoparticles remained homogeneous for at least 3 months and displayed desirable fluorescence quantum yields.

## ASSOCIATED CONTENT

**S Supporting Information.** Characterization data for the linear polymer of M1, <sup>19</sup>F NMR spectra of select systems, and spectral characterization data. This material is available free of charge via the Internet at <http://pubs.acs.org>.

## AUTHOR INFORMATION

### Corresponding Author

\*E-mail: [tswager@mit.edu](mailto:tswager@mit.edu)

## ACKNOWLEDGMENT

T.L.A. thanks the Chesonis Family Foundation for a graduate fellowship. The Biophysical Instrumentation Facility for the Study of Complex Macromolecular Systems (NSF-0070319 and NIH GM68762) is gratefully acknowledged.

## REFERENCES

- (1) Tuncel, D.; Demir, H. V. *Nanoscale* **2010**, *2*, 484.
- (2) (a) Kietzke, T.; Nehrer, D.; Landfester, K.; Montenegro, R.; Güntner, R.; Scherf, U. *Nature Mater.* **2003**, *2*, 408. (b) Mauthner, G.; Landfester, K.; Köck, A.; Brückl, H.; Kast, M.; Stepper, C.; List, E. J. W. *Org. Electron.* **2008**, *9*, 164. (c) Fisslthaler, E.; Blümel, A.; Landfester, K.; Scherf, U.; List, E. J. W. *Soft Matter* **2008**, *4*, 2448.
- (3) (a) Wu, C.; Szymanski, C.; Cain, Z.; McNeill, J. J. *Am. Chem. Soc.* **2007**, *129*, 12904. (b) Zhu, M.-Q.; Zhu, L.; Han, J. J.; Wu, W.; Hurst,

J. K.; Li, A. D. Q. *J. Am. Chem. Soc.* **2006**, *128*, 4303. (c) Tian, Z.; Wu, W.; Wan, W.; Li, A. D. Q. *J. Am. Chem. Soc.* **2009**, *131*, 4245. (d) Zhu, L.; Wu, W.; Zhu, M.-Q.; Han, J. J.; Hurst, J. K.; Li, A. D. Q. *J. Am. Chem. Soc.* **2007**, *129*, 3524. (e) Moon, J. H.; McDaniel, W.; MacLean, P.; Hancock, L. F. *Angew. Chem., Int. Ed.* **2007**, *46*, 8223.

(4) (a) Wu, C.; Szymanski, C.; McNeill, J. *Langmuir* **2006**, *22*, 2956. (b) Szymanski, C.; Wu, C.; Hooper, J.; Salazar, M. A.; Perdomo, A.; Dukes, A.; McNeill, J. *Phys. Chem. B* **2005**, *109*, 8543. (c) Wu, C.; McNeill, J. *Langmuir* **2008**, *24*, 5855.

(5) (a) Zhuang, D.; Hogen-Esch, T. E. *Macromolecules* **2010**, *43*, 8170. (b) Piok, T.; Gamerith, S.; Gadermaier, C.; Plank, H.; Wenzl, F. P.; Patil, S.; Montenegro, R.; Kietzke, T.; Nehrer, D.; Scherf, U.; Landfester, K.; List, E. J. W. *Adv. Mater.* **2003**, *15*, 800. (b) Kietzke, T.; Nehrer, D.; Kumke, M.; Montenegro, R.; Landfester, K.; Scherf, U. *Macromolecules* **2004**, *37*, 4882.

(6) (a) Grigalevicius, S.; Forster, M.; Ellinger, S.; Landfester, K.; Scherf, U. *Macromol. Rapid Commun.* **2006**, *27*, 200. (b) Wu, C.; Peng, H.; Jiang, Y.; McNeill, J. J. *Phys. Chem. B* **2006**, *110*, 14148.

(7) (a) Landfester, K.; Montenegro, R.; Scherf, U.; Güntner, R.; Asawapirom, U.; Patil, S.; Neher, D.; Kietzke, T. *Adv. Mater.* **2002**, *14*, 651. (b) Landfester, K. *Annu. Rev. Mater. Res.* **2006**, *36*, 231. (c) Müller, K.; Klapper, M.; Müllen, K. *Macromol. Rapid Commun.* **2006**, *27*, 586. (d) Berkefeld, A.; Mecking, S. *Angew. Chem., Int. Ed.* **2006**, *45*, 6044. (e) Baier, M. C.; Huber, J.; Mecking, S. *J. Am. Chem. Soc.* **2009**, *131*, 14267. (f) Pecher, J.; Mecking, S. *Macromolecules* **2007**, *40*, 7733.

(8) (a) Zollinger, H. *Color Chemistry*, 3rd ed.; VCH: Weinheim, 2003. (b) Würthner, F. *Chem. Commun.* **2004**, 1564.

(9) (a) Smart, B. E. In *Organofluorine Chemistry Principles and Commercial Applications*; Banks, R. E., Smart, B. E., Tatlow, J. C., Eds.; Plenum Press: New York, 1994; p 73. (b) Bartlett, P. D.; Montgomery, L. K.; Seidel, B. J. *J. Am. Chem. Soc.* **1964**, *86*, 616. (c) Spraul, B. K.; Suresh, S.; Jin, J.; Smith, D. W., Jr. *J. Am. Chem. Soc.* **2006**, *128*, 7055.

(10) (a) Smith, D. W., Jr.; Chen, S.; Kumar, S.; Ballato, J.; Shah, H.; Topping, C.; Foulger, S. *Adv. Mater.* **2002**, *14*, 1585. (b) Jin, J.; Smith, D. W., Jr.; Topping, C.; Suresh, S.; Chen, S.; Foulger, S.; Rice, N.; Mojazza, B. *Macromolecules* **2003**, *36*, 9000. (c) Jin, J.; Topping, C.; Suresh, S.; Foulger, S.; Rice, N.; Mojazza, B.; Smith, D. W., Jr. *Polymer* **2005**, *46*, 6923. (d) Smith, D. W., Jr.; Babb, D. A. *Macromolecules* **1996**, *29*, 852.

(11) (a) Neilson, A. R.; Budy, S. M.; Ballato, J. M.; Smith, D. W., Jr. *Macromolecules* **2007**, *40*, 9378. (b) Iacono, S. T.; Budy, S. M.; Moody, J. D.; Smith, R. C.; Smith, D. W., Jr. *Macromolecules* **2008**, *41*, 7490. (c) Spraul, B. K.; Suresh, S.; Glaser, S.; Perahia, D.; Smith, D. W., Jr. *J. Am. Chem. Soc.* **2004**, *126*, 12773.

(12) (a) Ma, H.; Jen, A. K.-Y.; Dalton, L. R. *Adv. Mater.* **2002**, *14*, 1339. (b) Budy, S. M.; Suresh, S.; Spraul, B. K.; Smith, D. W., Jr. *J. Phys. Chem. C* **2008**, *112*, 8099.

(13) Kang, S. H.; Luo, J.; Ma, H.; Barto, R. R.; Frank, C. W.; Dalton, L. R.; Jen, A. K.-Y. *Macromolecules* **2003**, *36*, 4355.

(14) (a) Carlson, B.; Phelan, G. D.; Kaminsky, W.; Dalton, L. R.; Jiang, X.; Liu, S.; Jen, A. K.-Y. *J. Am. Chem. Soc.* **2002**, *124*, 14162. (b) Niu, Y.-H.; Tung, Y.-L.; Chi, Y.; Shu, C.-G.; Kim, J. H.; Chen, B.; Luo, J.; Carty, A. J.; Jen, A. K.-Y. *Chem. Mater.* **2005**, *17*, 3532.

(15) Qiu, W.; Chen, S.; Sun, X.; Liu, Y.; Zhu, D. *Org. Lett.* **2006**, *8*, 867.

(16) A mixture of the 1,6- and 1,7-dibrominated PDI isomers was obtained following published procedures: (a) Zhan, X.; Tan, Z.; Domercq, B.; An, Z.; Zhang, X.; Barlow, S.; Li, Y.; Zhu, D.; Kippelen, B.; Marder, S. R. *J. Am. Chem. Soc.* **2007**, *129*, 7246. (b) Ahrens, M. J.; Fuller, M. J.; Wasielewski, M. R. *Chem. Mater.* **2003**, *15*, 2684. As previously reported, these isomers were difficult to separate by conventional purification methods: (c) Würthner, F.; Stepanenko, V.; Chen, Z.; Saha-Möller, C. R.; Kocher, N.; Stalke, D. *J. Org. Chem.* **2004**, *69*, 7933. A mixture of 1,6- and 1,7-dibromo isomers was used to synthesize **M3** (see note 17); however, compound **4** is shown as the 1,7-isomer in Scheme 1 for simplicity.

(17) Following multiple purifications by flash column chromatography, a sample that contained ca. 85% of the 1,7-isomer of **M3** (shown in Scheme 1) and ca. 15% of the 1,6-isomer was obtained, as determined from the <sup>1</sup>H NMR spectrum of the final mixture (see Supporting

Information). The chemical shifts of the 1,6- and 1,7-isomers were assigned based on previous assignments made for similar PDIs (see note 16).

(18) (a) Li, X.-Q.; Zhang, X.; Ghosh, S.; Würthner, F. *Chem.—Eur. J.* **2008**, *14*, 8074. (b) Nolde, F.; Qu, J.; Kohl, C.; Pschirer, N. G.; Reuther, E.; Müllen, K. *Chem.—Eur. J.* **2005**, *11*, 3959. (c) Weil, T.; Reuther, E.; Beer, C.; Müllen, K. *Chem.—Eur. J.* **2004**, *10*, 1398.

(19) Rose, A.; Tovar, J. D.; Yamaguchi, S.; Nesterov, E. E.; Zhu, Z.; Swager, T. M. *Philos. Trans. R. Soc. London, A* **2007**, *365*, 1589.

(20) Fluorescence quantum yields for **NP1–3** were measured against Rhodamine B in ethanol, which has a quantum yield of 0.71: Demas, J. N.; Crosby, G. A. *J. Phys. Chem.* **1971**, *75*, 991–1024. Fluorescence quantum yields for **NP4,5** were measured against zinc phthalocyanine in 1% pyridine in toluene, which has a quantum yield of 0.30: Vincett, P. S.; Voigt, E. M.; Rieckhoff, K. E. *J. Chem. Phys.* **1971**, *55*, 4131–4140.